

# Coherent artifact study of two-dimensional spectral shearing interferometry

MICHELLE RHODES,<sup>1,\*</sup> MADHURI MUKHOPADHYAY,<sup>1</sup> JONATHAN BIRGE,<sup>2</sup> AND RICK TREBINO<sup>1</sup>

<sup>1</sup>Georgia Institute of Technology, School of Physics, 837 State St NW, Atlanta, Georgia 30332, USA

<sup>2</sup>Lincoln Laboratory, Massachusetts Institute of Technology, 244 Wood Street, Lexington, Massachusetts 02420, USA

\*Corresponding author: mrhodes3@gatech.edu

Received 15 June 2015; revised 23 July 2015; accepted 24 July 2015; posted 24 July 2015 (Doc. ID 242984); published 14 August 2015

We study multi-shot intensity-and-phase measurements of unstable trains of ultrashort pulses using two-dimensional spectral shearing interferometry (2DSI). We find that, like other interferometric ultrashort-laser pulse-measurement methods, it measures only the coherent artifact and so yields effectively only a lower bound to the pulse length. We also attempt to identify warning signs of pulse-shape instability in 2DSI and find that it responds to instability with reduced fringe visibility, although this effect is very small when using the small spectral shears appropriate for large temporal ranges. We conclude that 2DSI should be used with caution and large-shear measurements or alternative techniques should be used to verify the stability of the pulse train. © 2015 Optical Society of America

**OCIS codes:** (320.0320) Ultrafast optics; (320.7080) Ultrafast devices; (320.7100) Ultrafast measurements.

<http://dx.doi.org/10.1364/JOSAB.32.001881>

## 1. INTRODUCTION

It is fundamentally impossible for any multi-shot measurement of an unstable quantity to yield a truly accurate result. For an unstable quantity, the multi-shot measurement involves contributions from an ensemble of different events. This is especially problematic because this ensemble measurement may not yield the average of the quantity being measured. In particular, any technique for measuring ultrashort-laser pulse trains with pulse-shape instabilities is doomed to fail, as a single pulse shape can never correctly describe the (possibly large) collection of different pulse shapes that contributed to the measurement. Because single-shot measurements are difficult to perform with most laser sources due to low pulse energies and long camera integration times, it is important for a pulse-measurement method to yield a reasonable average result. Further, it is very important that the method indicate whether its measurement averages over different events versus identical events. This problem is particularly important for trains of ultrashort pulses because even typically stable lasers are sensitive to a variety of fluctuations, including pump-laser power variations and, when misaligned, acoustic vibrations, which occur on time scales considerably shorter than typical camera integration times.

Although it is clear that averaged, multi-shot measurements are problematic if the pulse train being measured is unstable, this effect has not received the attention it deserves in ultrashort pulse measurement. In 1969, Fisher and Fleck first identified this issue in multi-shot intensity autocorrelation measurements, describing and explaining the classic spike-and-pedestal-shaped

trace that is typical of averaging over variably shaped complex pulses [1]. In this case, the average pulse length is best indicated by the width of the pedestal in the averaged autocorrelation trace, not the width of the coherence spike. Unfortunately, several decades later, misinterpretations of the coherence spike in autocorrelation continue [2].

Autocorrelation's problems are more deeply rooted, however, as the shape of the autocorrelation is not at all a robust indicator of the pulse shape [3]. Interestingly, it has been shown that the shape of a multi-shot autocorrelation is actually more sensitive to the shape of a distribution of pulse widths than to the profile of individual pulses [4]. In any case, autocorrelation is now generally considered obsolete for many applications in view of newer, more powerful, and informative methods that yield the complete temporal intensity and phase of the pulse. Unfortunately, with only one exception to our knowledge [5,6], pulse-shape instability has not been considered in most of these newer methods until very recently. Indeed, reliability metrics and sometimes even error estimation have been absent from ultrashort pulse measurements for far too long, and one consequence is that the warning signs of pulse-shape instability are unknown for most of these newer pulse-measurement techniques.

Most of these more advanced pulse-measurement methods also yield results that are very different from average pulses in the presence of pulse-shape instability, and this poor performance has only recently been identified for several of them. In recent publications, the effects of pulse-shape instability

on measurement results have been studied for several ultrashort pulse-measurement techniques: frequency-resolved optical gating (FROG) [7,8], spectral interferometry for direct electric field reconstruction (SPIDER) [9,10], and self-referenced spectral interferometry (SRSI) using cross-polarized wave generation [11,12].

Techniques that measure only the stable or repeatable part of a pulse train and do not reflect the variations are said to measure only the coherent artifact. In particular, interferometric measurements that rely on fringes to retrieve pulse information are especially susceptible to retrieving only a coherent artifact. Because the interferometric measurement process ignores variations, the averaged measurement yields a pulse that is quite different from an average pulse. This is the case for both SPIDER [13,14] and SRSI [15]. Phase variations cause fringes to wash out, and the remaining averaged fringes (with reduced visibility) represent only the stable component of the pulse train. The unstable component information resides only in the background. In effect, SPIDER does what it is supposed to do: measure the average spectral phase, which, in the presence of fluctuations, is significantly less complex than that of a single pulse in the train and usually flat. But a flat spectral phase corresponds to the shortest pulse for a given spectrum—the definition of the coherent artifact. For SPIDER, the resulting increased background is generally the only indicator of instability, but other benign causes of background, such as slight device misalignment, also exist, and it is difficult to separate them out. Since there is no independent “stability meter” for pulse shapes in trains of ultrashort laser pulses, it is very important that there be a reliable way to distinguish a train of stable, short, and simple pulses from a train of unstable, long, and complex pulses. While SRSI retrieves a coherent artifact, it is much more able to distinguish unstable pulse trains from stable ones. SRSI has an internal cross-check that is violated for unstable pulse trains: the spectrum of the pulse generated in it via cross-polarized wave generation should be the same in the measurement as when calculated from the retrieved pulse [15,16]. So it yields an indication of pulse-train instability when its cross-check is used.

Fortunately, a FROG measurement, whose two-dimensional traces massively over-determine the pulse, yields a noticeably high rms error between measured and retrieved traces (known as the FROG error) when confronted with an unstable pulse train. Since comparing measured and retrieved FROG traces is standard practice, this is an excellent indicator of instability. Different versions of FROG perform differently in regard to retrieving the average structure in the pulse intensity and spectrum, but FROG's retrieved pulses generally reasonably reflect the approximately correct full width at half-maximum pulse length, even in the presence of significant instability [13,14]. As a result, FROG is currently the only known intensity-and-phase measurement method that does not measure only a coherent artifact.

Here, we consider these issues for the intensity-and-phase measurement technique, two-dimensional spectral shearing interferometry (2DSI) [17,18]. We also consider whether it provides an indication of the stability of the pulse train or otherwise indicates the reliability of its measurement. In order

to do this, we study its response to trains of unstable pulses. Ideally, we will identify a method of distinguishing between stable and unstable pulse trains in measured 2DSI traces. This is of particular interest because 2DSI is quite closely related to SPIDER, which has already been shown to measure only the coherent artifact and so cannot distinguish simple, short, and stable pulse trains from complicated, long, and unstable ones [13,14].

## 2. BACKGROUND

2DSI and SPIDER are both based on interfering pulse replicas with slightly different center frequencies to determine the spectral phase of pulses. The difference in center frequency between the pulse replicas is referred to as the shear. Spectrally shearing one of the replicas means that the difference in spectral phase between frequencies separated by the shear affects the signal, allowing the phase to be reconstructed. In SPIDER, the pulse replicas have a relative delay, creating spectral fringes that are modulated by the difference in phase [see Fig. 1(a)]. The ideal SPIDER signal, in terms of the spectrum  $S(\omega)$ , spectral phase  $\varphi(\omega)$ , frequency shear  $\Omega$ , and delay  $T$ , is

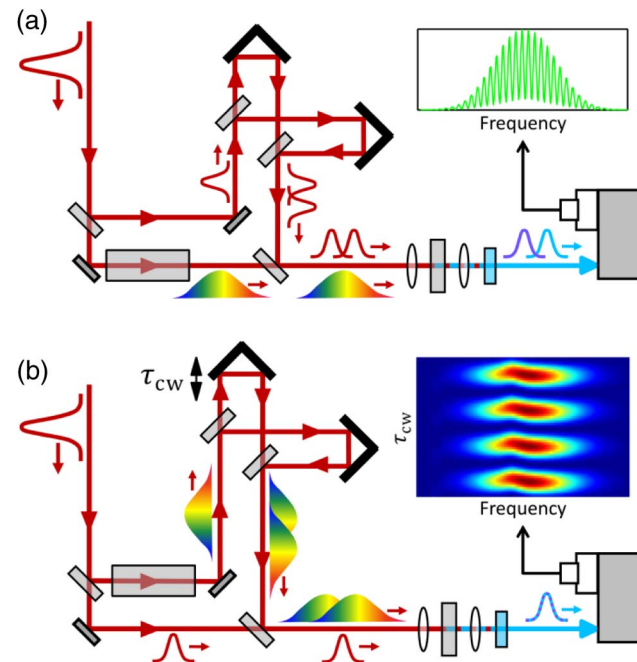


**Fig. 1.** Basic schematic of (a) SPIDER and (b) 2DSI. The delay lines necessary to maintain the correct relative delay between chirped and nonchirped pulses are omitted for simplicity. We show a dispersive medium being used to generate chirped pulses, but a prism or grating and a mirror may be used instead. Pulse replicas interact in a sum-frequency-generation crystal and are measured by a spectrometer after a filter removes the fundamental light. In a SPIDER measurement, the relative delay between pulse replicas generates spectral fringes which are modulated by the local group delay. In a 2DSI measurement, scanning the delay between chirped pulse replicas creates fringes in the delay direction which are similarly modulated by the local group delay.

$$\begin{aligned} S_{\text{SPIDER}}(\omega) = & S(\omega) + S(\omega - \Omega) \\ & + 2\sqrt{S(\omega)S(\omega - \Omega)} \cos[\omega T + \varphi(\omega) - \varphi(\omega - \Omega)]. \end{aligned} \quad (1)$$

To create this signal, two pulse replicas interact in a nonlinear crystal with different portions of a significantly chirped pulse. The difference in frequency between these portions creates the spectral shear. Sum-frequency generation is the typical nonlinear interaction, but difference-frequency generation works equally well and may be preferable for some wavelengths.

2DSI differs from SPIDER in that it uses pulse replicas that overlap exactly in time but have a small relative phase offset in addition to the frequency shear [see Fig. 1(b)]. This is accomplished by allowing a single pulse replica to interact with different portions of two significantly chirped pulses. The delay between the chirped pulses sets the spectral shear. A phase offset between the resulting higher-frequency pulse replicas is created by varying the delay between the quasi-CW beams very slightly. Scanning the phase offset through several electric field cycles and recording the resulting spectrum at each delay produces a two-dimensional plot with several visible fringes in the delay direction. An expression for the ideal 2DSI signal is

$$\begin{aligned} S_{\text{2DSI}}(\omega, \tau_{\text{cw}}) = & S(\omega) + S(\omega - \Omega) \\ & + 2\sqrt{S(\omega)S(\omega - \Omega)} \cos[\omega\tau_{\text{cw}} + \varphi(\omega) - \varphi(\omega - \Omega)], \end{aligned} \quad (2)$$

where  $\tau_{\text{cw}}$  is the phase offset. As in SPIDER, one can make the approximation that the phase difference in the cosine term is approximately the group delay (the derivative of the phase) times the shear or

$$\begin{aligned} S_{\text{2DSI}}(\omega, \tau_{\text{cw}}) \approx & S(\omega) + S(\omega - \Omega) \\ & + 2\sqrt{S(\omega)S(\omega - \Omega)} \cos[\omega\tau_{\text{cw}} + t_g(\omega)\Omega], \end{aligned} \quad (3)$$

where  $t_g(\omega)$  is the group delay. The fringe at each frequency will be offset according to the group delay at that frequency. Consequently, the group delay can be obtained by Fourier transforming the signal along the phase/delay direction and taking the phase of either AC sideband. The group delay can then be integrated to determine the spectral phase as in SPIDER.

We have mentioned that the effect of pulse-shape instability on a SPIDER measurement is to reduce the fringe visibility. This occurs due to variations in the group delay. The group-delay term in Eq. (3) controls the offset of the sinusoidal fringe pattern at each frequency. If the group delay changes, the fringes move. Thus, averaging over many pulses with different group delays means that the fringes begin to wash out, resulting in lower peaks and higher troughs. We will refer to “fringe visibility” in this paper, numerically defined as one minus the ratio of the highest trough (or background) to the highest fringe peak. A measurement with no background, whose troughs have a peak value of zero, has 100% fringe visibility.

In the typical equations for SPIDER and 2DSI above, the stretched pulses used in the measurement are assumed to be essentially continuous-wave beams of the desired frequency. This assumption is reasonable for measuring short pulses with fairly flat phases. In the general case, however, considering

sum-frequency generation with stretched pulses instead of CW beams significantly complicates the mathematics involved. These effects may very well be important, especially when considering averaging over many different pulses. The simplest correction to the above equations is to consider the impact of a difference in phase between different colors in the pulse. Generally speaking, the spectral phase is not flat and any two frequencies will have a nonzero phase difference. When the pulse is stretched, these two colors will retain their original phase difference in addition to any phase difference caused by chirping. Even if we assume that the chirp is symmetrical, such that it does not introduce any additional relative phase, the pulse replicas will still inherit the relative spectral phase of the two upconverting frequencies. If the spectral phase varies from pulse to pulse, then the relative phase of the pulse replicas will vary as well. The effect of these variations is to shift the fringes from shot to shot. We expect this to further decrease the fringe visibility in simulated unstable-train measurements, in addition to the reduction in fringe visibility already expected from group-delay variations as discussed in the previous paragraph.

### 3. METHODS

The effects of pulse-shape variation on a measurement are easily simulated. The first step is to generate semi-random pulse trains with a stable component that is the same from pulse to pulse and an unstable component that varies. For this study, we use pulse trains that have been used to study other pulse-measurement methods [14,15]. These trains consist of 5000 pulses whose stable components are simple flat-phase Gaussians. The unstable components are time-gated thermal-emission-type noise (that is, a given spectrum with a random spectral phase for each frequency, as one would expect in the absence of mode-locking) with the same average spectrum as the stable component. The width of the time-gating function controls the average length and complexity of the pulses.

Starting with a Gaussian with a pulse length of  $20\delta t$  on a grid of 4096 time points (where  $\delta t$  is an arbitrary time unit), we use discrete Fourier transform relations to define the frequency sampling as  $\delta\omega = 2\pi/4096\delta t$ , implying that the corresponding bandwidth of the pulse must be  $90\delta\omega$ . This pulse functions as the stable component of the pulse trains and defines the spectrum of the thermal noise. We adjust the time-gating function applied to the thermal noise to make one pulse train with an average full width at half-maximum (FWHM) pulse length of  $59\delta t$  and average time-bandwidth product (TBP) of 2.7 and second train with an average pulse length of  $192\delta t$  and an average TBP of 9.1.

A 2DSI measurement of each pulse train was simulated for two different frequency shears. The larger shear ( $9\delta\omega$ ) corresponds to 10% of the FWHM bandwidth of the pulses. The smaller shear ( $4\delta\omega$ ) corresponds to 4% of the FWHM bandwidth. The simulated traces were created with 16 delay increments per electric field cycle, with 4 full cycles. Although 2DSI is an inherently multi-shot technique, the averaged measurement is simulated with each pulse contributing to the signal at each delay. We treat the measurement as an ergodic process in which averaging over time is equivalent to averaging

the whole trace over a large number of pulses. This is consistent with typical oscillator repetition rates compared to delay stage scan rates. However, if very few pulses are used to generate the signal at each delay or if there is some systematic drift in the laser source, then it is possible that the trace may not be periodic with respect to phase offset. If this happens, it is a very clear indicator of pulse-shape instability.

The number of pulses in each train (5000) is chosen to be relatively consistent with common experimental practice. Typical cameras have an exposure time of the order of tenths of a second, meaning that even kilohertz-rep-rate systems can average over several hundred pulses in a single frame, and the more common megahertz-rep-rate systems average over considerably more than 5000 pulses.

To determine what other features may signify that the pulse train being measured is unstable, the simulation of an average measurement over an unstable train of pulses is compared to a simulation of the measurement of the stable pulse component alone. Ideally, the measured spectral phase for the unstable train would be different from the stable train, somehow reflecting the properties of the unstable pulse component. However, even if the retrieved spectral phase is the same for both, any differences in the raw measurement would signal that the pulse train being measured is not stable. To explore how important the approximations are, we have simulated these 2DSI measurements both using a CW-beam-type simulation (where the spectral phase does not affect the upconverting beams) and the small correction that includes the relative phase of the upconverting frequencies.

## 4. RESULTS AND DISCUSSION

The simulated measurements of the pulse trains using 2DSI without the relative phase correction are shown in Fig. 2. Notice that all of the simulated measurements yield a flat spectral phase, which is the frequency-domain equivalent of the coherent artifact. Applying this flat phase to the separately measured average spectrum yields a pulse with the same temporal width as the stable component of the pulse train. This means that, in most cases, 2DSI measures only the stable component of an unstable pulse train—the coherent artifact. The measurement result does not reflect any of the variations between the pulses.

The one clear difference between the measurements of the unstable trains and the measurement of the stable train is the difference in fringe visibility. There is appreciable background in the measurements of the longer unstable pulse train, which is very obvious when using a large shear. The reason for larger shears yielding worse fringe visibility is apparent from Eq. (3): the fringes are shifted by an amount equal to the group delay multiplied by the spectral shear. Variations in the group delay due to pulse-shape instability cause the fringes to change position from shot to shot. The larger shear causes more fringe movement and therefore worse fringe visibility. This also explains why the fringe visibility is worse for the more complicated pulse train. This train has more, larger variations in the group delay, also causing more fringe displacement. All of these trends are repeated for the simulations with the relative-phase correction, shown in Fig. 3. As expected, the backgrounds are generally larger and the fringe visibility is generally worse.

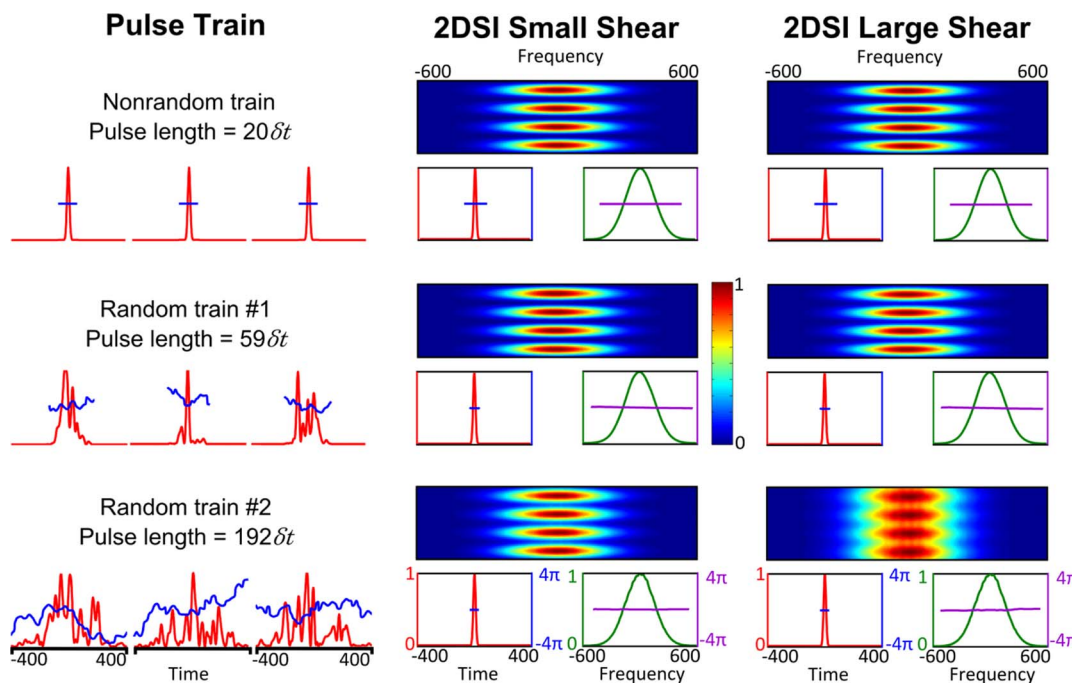


**Fig. 2.** Coherent artifact simulation for 2DSI using CW beams to upconvert. Example pulses from the unstable pulse train are given in the left column. The measurement and retrieved temporal and spectral intensity and phase are in the middle and right column. (Red is temporal intensity, blue is temporal phase, dark green is spectral intensity, and purple is spectral phase.) Measurements in the middle column use a small frequency shear: 4% of the FWHM pulse bandwidth. The fringe visibility is 98% for the  $59\delta t$  train and 78% for the  $192\delta t$  train (backgrounds of 2% and 22%, respectively). Measurements in the right column use a larger frequency shear: 10% of the FWHM pulse bandwidth. The fringe visibility is 90% for the  $59\delta t$  train and 23% for the  $192\delta t$  train (backgrounds of 10% and 77%, respectively).

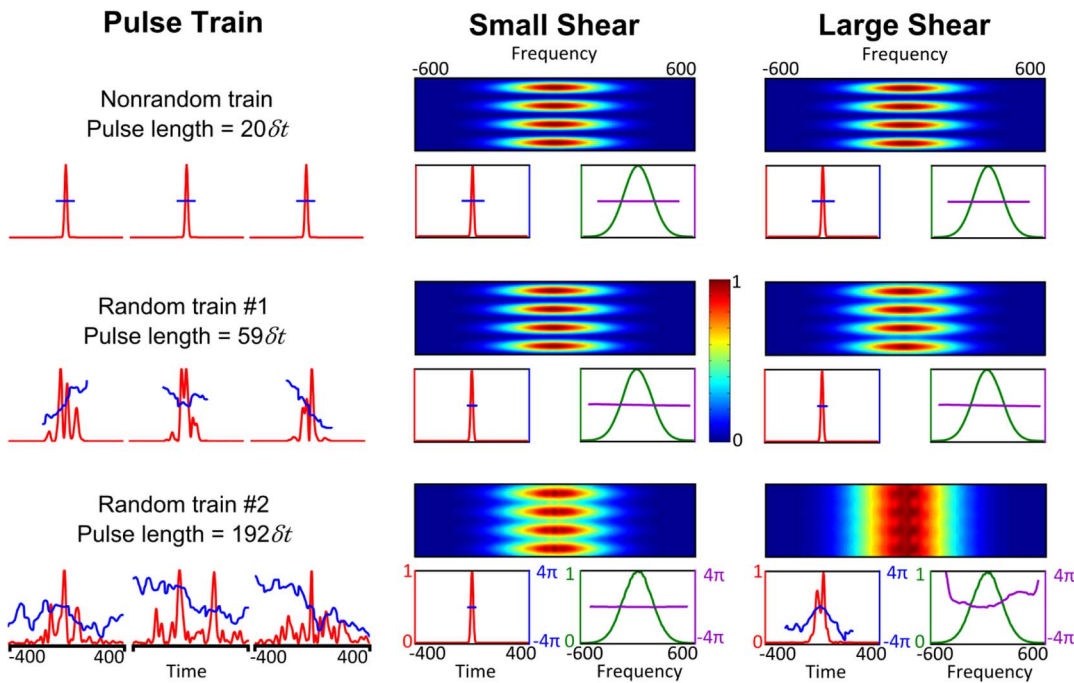
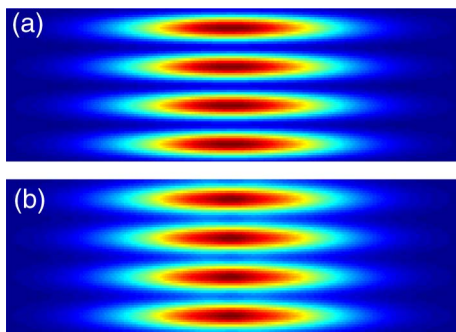


**Fig. 3.** Coherent artifact simulation for 2DSI taking into account the relative spectral phase of upconverting frequencies. Measurements in the middle column use a small frequency shear: 4% of the FWHM pulse bandwidth. The fringe visibility is 94% for the  $60\delta t$  train and 49% for the  $192\delta t$  train (backgrounds of 6% and 51%, respectively). Measurements in the right column use a larger frequency shear: 10% of the FWHM pulse bandwidth. The fringe visibility is 76% for the  $60\delta t$  train and 3% for the  $192\delta t$  train (backgrounds of 24% and 97%, respectively).

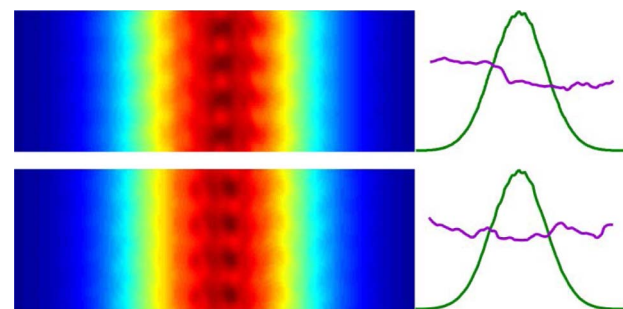
Interestingly, the background for the shorter unstable pulse train increases much more when using a larger shear in this simulation (see Fig. 4 for direct comparison). This means that using the background as an indicator of instability should be more robust than is suggested by the simpler simulation. However, most of the measurements still produce fringes that indicate a flat spectral phase and hence only a coherent artifact. The exception to this generalization is the larger shear measurements of the more complicated pulse train with the relative phase correction. In this case, the fringes are nearly nonexistent, with the background reaching 97% of the peak fringe visibility. It is abundantly clear that this measurement represents a highly unstable pulse train. However, the retrieved spectral phase is not particularly indicative of the characteristics of the pulse

train. In fact, the retrieved phase changes if we choose different frequencies (still separated by the same shear) to upconvert the pulse (see Fig. 5).

Making a measurement that averages over significantly fewer pulses still results in fairly flat spectral phases and short retrieved pulses. Figure 6 shows the results of averaging over 10, 50, and 200 pulses from random train number 1 (instead of all 5000) for both small and large shears, including the relative phase correction. For a small number of pulses with the type of variations we consider here, the average spectrum is significantly different from the average spectrum of the whole pulse train. Despite this, the measured spectral phase is quite flat. Therefore, the retrieved pulses are quite short and simple in the time domain. Comparing trace (a) and trace (d) clearly



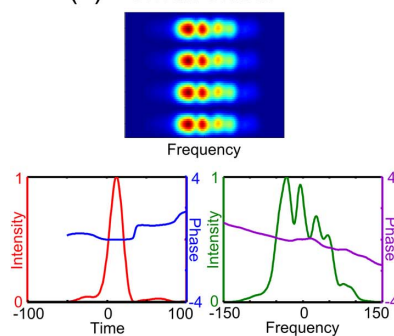
**Fig. 4.** Direct comparison of fringe visibility for large-shear measurements of the  $59\delta t$  pulse train (a) without and (b) with the relative phase correction. The background is 10% in (a) and 24% in (b).



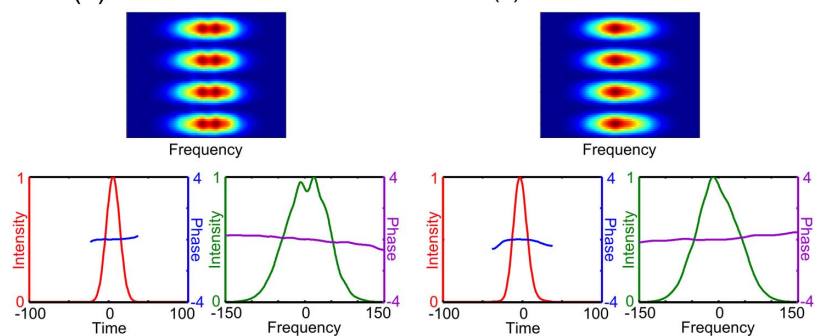
**Fig. 5.** Examples of different spectral phases (purple line, right) retrieved from traces (left) of the longer pulse train using different pairs of frequencies in the chirped pulses to generate the same large shear. A third example is in the bottom-right corner of Fig. 3.

**10 Pulse Average**

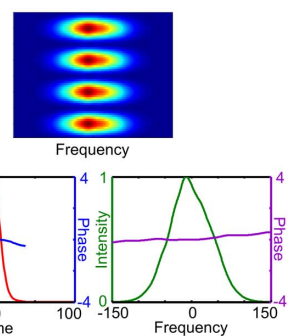
(a) Small Shear

**50 Pulse Average**

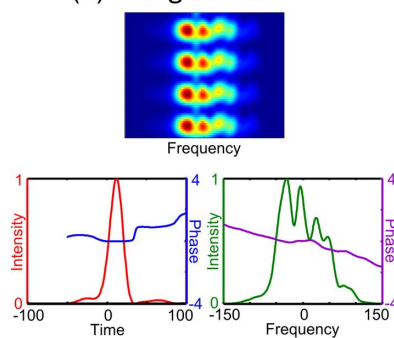
(b) Small Shear

**200 Pulse Average**

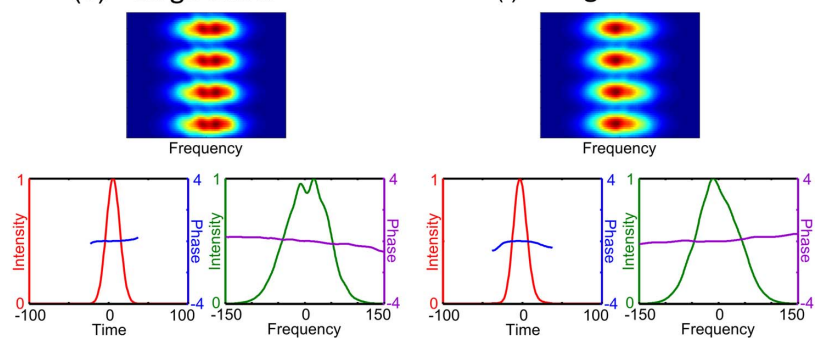
(c) Small Shear



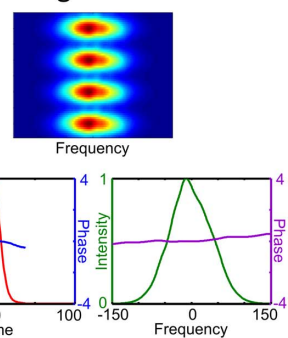
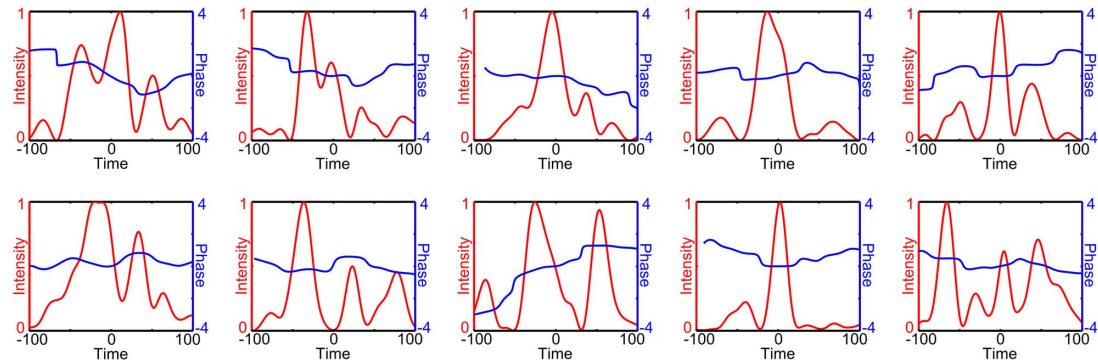
(d) Large Shear



(e) Large Shear



(f) Large Shear

**Actual Pulses**

**Fig. 6.** Coherent artifact simulation for 2DSI considering a small number of pulses taken from random train number 1. The top row shows traces created with a small spectral shear: 4% of the pulse bandwidth. The middle row shows traces created with a larger shear: 10% of the pulse bandwidth. The bottom rows show the temporal intensity and phase of the ten pulses averaged over in traces (a) and (d). Trace (a) has 97% fringe visibility and 3% background. Traces (b) and (c) have 94% fringe visibility and 6% background. Traces (d) and (e) have 78% fringe visibility and 22% background. Trace (f) has 76% fringe visibility and 24% background.

shows the increased fringe displacement that occurs for larger shear values. The retrieved spectral phase is identical for both shears in all cases. The lower part of Fig. 6 shows the ten pulses that contributed to the average in parts (a) and (d). These pulses are clearly rather long and complicated, in stark contrast to their average measurement. The lesson is clear: averaging over only a few pulses does not protect one from making a very wrong measurement in the presence of serious instability.

The fringe visibility in (a) is quite high at 97%, only showing a 3% background. Interestingly, the background in (d) is

22%, which is only slightly lower than the 24% background present in the large-shear, full 5000-pulse average of that pulse train. When averaging over 50 or more pulses, the spectral phase is entirely flat and adding additional pulses mainly serves to even out the average spectrum. The background in the small-shear traces (b) and (c) is 6%, consistent with the small-shear measurement of the full train. Likewise, the backgrounds in (e) and (f) are 22% and 24%, respectively. Aside from the shape of the average spectrum, these measurements of 50 pulses are essentially the same as the corresponding measurements of 5000 pulses.

Of course, when not working in the limit of averaging over many pulses, the exact characteristics and behavior of the pulse-to-pulse variations have a large impact on the results. One can therefore expect the threshold at which the average measured phase becomes flat to change based on the type and strength of the variations considered. Nevertheless, it is clear that it is possible for a measurement of only a few pulses to be quite wrong.

Based on our simulations, we conclude that considering the impact of spectral phase on the chirped pulses is informative and important when the spectral phase varies appreciably. Of course, the reality of using stretched pulses as quasi-CW beams to generate spectrally sheared replicas is even more complicated than the simple correction considered here. However, it is important to keep in mind that the viability of this measurement technique depends on having a suitably accurate mathematical description of the physical nonlinear measurement. If too many adjustments to the model are required to correctly model the experiment, then there are serious theoretical problems with the measurement technique.

In this case, further corrections or a full-field simulation are unlikely to result in better fringe visibility. In addition, many other causes of reduced fringe visibility are likely to remain consistent in measurements with different spectral shears, while the fringe visibility caused by instability becomes distinctly more pronounced with large shears. We can therefore conclude that the presence of background in a large-shear 2DSI measurement is an effective warning of pulse-shape instability.

However, using large shears in spectral shearing techniques can yield less accurate results because the measurement effectively samples the group delay of the pulse more sparsely [19]. One consequence is that the assumption of the phase difference being approximately the group delay times the shear, used to transform Eq. (1) into Eq. (2), becomes less accurate. Higher-order terms in the expansion of the phase become more important and dropping them introduces larger errors for large shears.

Fortunately, the frequency shear in 2DSI is an independent parameter that can be adjusted without changing other measurement parameters, by simply changing the delay between the chirped pulses. A standard SPIDER setup does not have this flexibility, because the spectral shear and the delay between the pulses cannot be changed separately without also altering the amount of chirp applied to the stretched pulse. This makes it harder to do a direct comparison and makes it less likely that any background due to benign alignment issues will be consistent between measurements with different shears. There are several other SPIDER variants besides 2DSI that are able to easily adjust the spectral shear. In particular, in the absence of spatiotemporal distortions, spatially encoded arrangement (SEA) SPIDER [20] traces are essentially equivalent to the 2DSI traces shown in this paper, and the discussion presented above will also apply directly to that technique. When the spectral shear is an independent measurement parameter, it is simple to make a large-shear measurement to verify the stability of the pulse train in addition to making a small-shear measurement to better estimate the spectral phase of the pulse. This has other beneficial implications: it has been shown that spectral phase measurements taken at different shears can be

combined to improve the overall accuracy of the retrieved spectral phase [19].

## 5. CONCLUSIONS

In conclusion, 2DSI generally retrieves only a coherent artifact when confronted with unstable pulse trains, but it can successfully warn users of very unstable pulse trains. This requires the extra step of taking a measurement with a large frequency shear to ensure that the fringe visibility is still good. In the absence of this additional information, however, 2DSI can misrepresent an unstable train of complicated pulses as a stable train of simple pulses. In addition, small variations might remain undetected even with an additional measurement. Consequently, this information should always be presented unless the stability of the source has been convincingly guaranteed in some other fashion.

**Funding.** Georgia Research Alliance (GRA); National Science Foundation (NSF) (ECCS-1307817).

## REFERENCES

1. R. A. Fisher and J. J. A. Fleck, "On the phase characteristics and compression of picosecond light pulses," *Appl. Phys. Lett.* **15**, 287–290 (1969).
2. K. G. Wilcox and A. C. Tropper, "Comment on SESAM-free mode-locked semiconductor disk laser," *Laser Photon. Rev.* **7**, 422–423 (2013).
3. E. Ippen and C. Shank, "Techniques for measurement," in *Ultrashort Light Pulses*, S. Shapiro, ed. (Springer, 1977), pp. 83–122.
4. E. W. Van Stryland, "The effect of pulse to pulse variation on ultrashort pulselwidth measurements," *Opt. Commun.* **31**, 93–96 (1979).
5. X. Gu, L. Xu, M. Kimmel, E. Zeek, P. O'shea, A. P. Shreenath, R. Trebino, and R. S. Windeler, "Frequency-resolved optical gating and single-shot spectral measurements reveal fine structure in microstructure-fiber continuum," *Opt. Lett.* **27**, 1174–1176 (2002).
6. J. Dudley, X. Gu, L. Xu, M. Kimmel, E. Zeek, P. O'shea, R. Trebino, S. Coen, and R. Windeler, "Cross-correlation frequency resolved optical gating analysis of broadband continuum generation in photonic crystal fiber: simulations and experiments," *Opt. Express* **10**, 1215–1221 (2002).
7. R. Trebino, *Frequency-Resolved Optical Gating: The Measurement of Ultrashort Laser Pulses* (Kluwer/Academic, 2002).
8. R. Trebino, K. W. DeLong, D. N. Fittinghoff, J. N. Sweetser, M. A. Krumbügel, B. A. Richman, and D. J. Kane, "Measuring ultrashort laser pulses in the time-frequency domain using frequency-resolved optical gating," *Rev. Sci. Instrum.* **68**, 3277–3295 (1997).
9. C. Iaconis and I. A. Walmsley, "Spectral phase interferometry for direct electric-field reconstruction of ultrashort optical pulses," *Opt. Lett.* **23**, 792–794 (1998).
10. C. Iaconis and I. A. Walmsley, "Self-referencing spectral interferometry for measuring ultrashort optical pulses," *IEEE J. Quantum Electron.* **35**, 501–509 (1999).
11. T. Oksenhendler, S. Coudreau, N. Forget, V. Crozatier, S. Grabielle, R. Herzog, O. Gobert, and D. Kaplan, "Self-referenced spectral interferometry," *Appl. Phys. B* **99**, 7–12 (2010).
12. A. Moulet, S. Grabielle, C. Cornaggia, N. Forget, and T. Oksenhendler, "Single-shot, high-dynamic-range measurement of sub-15 fs pulses by self-referenced spectral interferometry," *Opt. Lett.* **35**, 3856–3858 (2010).
13. J. Ratner, G. Steinmeyer, T. C. Wong, R. Bartels, and R. Trebino, "Coherent artifact in modern pulse measurements," *Opt. Lett.* **37**, 2874–2876 (2012).
14. M. Rhodes, G. Steinmeyer, J. Ratner, and R. Trebino, "Pulse-shape instabilities and their measurement," *Laser Photon. Rev.* **7**, 557–565 (2013).

15. M. Rhodes, G. Steinmeyer, and R. Trebino, "Standards for ultrashort-laser-pulse-measurement techniques and their consideration for self-referenced spectral interferometry [Invited]," *Appl. Opt.* **53**, D1–D11 (2014).
16. T. Oksenhendler, "Self-referenced spectral interferometry theory," arXiv preprint arXiv:1204.4949 (2012).
17. J. R. Birge, R. Ell, and F. X. Kärtner, "Two-dimensional spectral shearing interferometry for few-cycle pulse characterization," *Opt. Lett.* **31**, 2063–2065 (2006).
18. J. R. Birge and F. X. Kärtner, "Analysis and mitigation of systematic errors in spectral shearing interferometry of pulses approaching the single-cycle limit [Invited]," *J. Opt. Soc. Am. B* **25**, A111–A119 (2008).
19. D. R. Austin, T. Witting, and I. A. Walmsley, "High precision self-referenced phase retrieval of complex pulses with multiple-shearing spectral interferometry," *J. Opt. Soc. Am. B* **26**, 1818–1830 (2009).
20. E. M. Kosik, A. S. Radunsky, I. A. Walmsley, and C. Dorner, "Interferometric technique for measuring broadband ultrashort pulses at the sampling limit," *Opt. Lett.* **30**, 326–328 (2005).